

 Open access • Journal Article • DOI:10.1002/PSSR.201206224

## Efficient second harmonic generation by birefringent phase matching in femtosecond-laser-inscribed KTP cladding waveguides — [Source link](#)

Ningning Dong, Feng Chen, J. R. Vázquez de Aldana

**Institutions:** Shandong University, University of Salamanca

**Published on:** 01 Jul 2012 - Physica Status Solidi-rapid Research Letters (John Wiley & Sons, Ltd)

**Topics:** Second-harmonic generation, Cladding (fiber optics), Femtosecond, Birefringence and Laser

Related papers:

- [Optical waveguides in crystalline dielectric materials produced by femtosecond-laser micromachining](#)
- [Writing waveguides in glass with a femtosecond laser](#)
- [Optically pumped planar waveguide lasers, Part I: Fundamentals and fabrication techniques](#)
- [Depressed cladding, buried waveguide laser formed in a YAG:Nd<sup>3+</sup> crystal by femtosecond laser writing](#)
- [Femtosecond-Laser-Inscribed BiB3O6 Nonlinear Cladding Waveguide for Second-Harmonic Generation](#)

Share this paper:    

View more about this paper here: <https://typeset.io/papers/efficient-second-harmonic-generation-by-birefringent-phase-1xk1fo1dz>

# Efficient second harmonic generation by birefringent phase matching in femtosecond-laser-inscribed KTP cladding waveguides

Ningning Dong<sup>1</sup>, Feng Chen<sup>\*1</sup>, and J. R. Vázquez de Aldana<sup>2</sup>

<sup>1</sup> School of Physics, State Key Laboratory of Crystal Materials and Key Laboratory of Particle Physics and Particle Irradiation (MOE), Shandong University, 250100 Jinan, P.R. China

<sup>2</sup> Laser Microprocessing Group, Universidad de Salamanca, 37008 Salamanca, Spain

Received 21 May 2012, revised 31 May 2012, accepted 1 June 2012

Published online 5 June 2012

**Keywords** optical cladding waveguides, second harmonic generation, femtosecond laser inscription, KTP crystals

\* Corresponding author: e-mail drfchen@sdu.edu.cn, Phone: +86 531 88363007, Fax: +86 531 88363350

We report on the fabrication of nonlinear  $\text{KTiOPO}_4$  (KTP) cladding waveguides by using femtosecond-laser direct inscription. The produced guiding structures with a circular cross section of  $\sim 100 \mu\text{m}$  diameter support good light confinement both for the visible and infrared, for TE and TM polarization. Under the 1064 nm pulsed fundamental pump beam, guided-wave second harmonic generation (SHG) at

532 nm has been realized with an optical conversion efficiency as high as 45.6% ( $\sim 0.076\% \text{ W}^{-1} \text{ cm}^{-2}$ ), which is three times the magnitude of the normalized efficiency obtained for “double-line” KTP waveguides (fabricated with the aim of comparison), thus showing an intriguing potential as integrated frequency converters.

© 2012 WILEY-VCH Verlag GmbH & Co. KGaA, Weinheim

**1 Introduction** Nonlinear optical waveguides play an important role in the promising on-chip-integrated micro photonic devices owing to the combination of nonlinear features of bulks and waveguide compact geometries [1, 2]. Potassium titanyl phosphate ( $\text{KTiOPO}_4$  or KTP) is a widely used nonlinear crystal for frequency conversion [3]. Compared with lithium niobate ( $\text{LiNbO}_3$ ), KTP possesses outstanding thermal robustness. KTP waveguides have been produced by ion exchange (e.g.,  $\text{Rb}^+ \leftrightarrow \text{K}^+$ ) [4] or by the implantation of energetic ions (e.g.,  $\text{He}^+$ ,  $\text{Li}^+$ ) [5–7]. Second harmonic generation (SHG) of green lasers was also realized in ion-exchanged periodically poled KTP (PPKTP) via quasi-phase-matching (QPM) [5] and in He-ion-implanted KTP waveguides through birefringent phase-matching (PM) configuration [5]. Since 1996 [8], femtosecond (fs) laser inscription has become a unique and powerful technique to fabricate waveguides in many optical materials and a wide range of photonic applications have been realized. These guiding structures are mainly the single-line writing waveguides (so-called Type I, with positive refractive index changes in the irradiated region) and stress-induced waveguides (so-called Type II, guiding regions usually exist

between two index-reduced irradiation tracks) [9, 10]. For fs-laser micromachined nonlinear crystals, efficient SHG has been realized in Type I  $\text{LiNbO}_3$  (PM) [11] and Type II  $\text{Nd}^{3+}:\text{YAB}$  [12], PPKTP [13] or PPLN (periodically poled  $\text{LiNbO}_3$ ) QPM waveguides [14]. For PM SHG, it is required that the waveguides support the analogous guidance of the fundamental and second harmonic (SH) waves (corresponding to the two orthogonal polarization directions, TE and TM, respectively). In this sense, the cladding waveguides produced by fs-laser inscription might be advantageous since the large-area cross sections may offer more homogeneous distributions of the fundamental and SH light fields, resulting in a more efficient overlap of the pump and SH profiles. This geometry has been realized in a few laser materials, e.g., Nd:YAG crystal [15] and Tm:ZBLAN glass [16]. In this Letter, we report on the fabrication of depressed cladding waveguides, supporting the two transverse polarizations in a KTP crystal by using the fs-laser inscription, and the efficient guided-wave PM SHG of 1064 nm pulsed pump light. A comparison of PM SHG performance between KTP cladding and stress-induced “double-line” (DL) waveguides is also presented.

**2 Experiments and results** The optically polished KTP crystal used in this work was cut into  $8 \times 10 \times 2 \text{ mm}^3$  to satisfy the Type II ( $e^\omega + o^\omega \rightarrow e^{2\omega}$ )  $1064 \rightarrow 532 \text{ nm}$  PM SHG (i.e.,  $\theta = 90^\circ$ ,  $\varphi = 23.5^\circ$ ) along the 8 mm axis. The cladding waveguides were fabricated by an amplified Ti:sapphire laser system generating linearly-polarized 120 fs pulses at a central wavelength of 795 nm and with a repetition rate of 1 kHz (1 mJ maximum pulse energy). The precise value of the pulse energy used to irradiate the sample was set with a calibrated neutral density filter, a half-wave plate and a linear polarizer. The sample was placed in a computer controlled motorized three-axes stage. The beam was focused through the largest sample surface (dimensions  $8 \times 10 \text{ mm}^2$ ) at a depth ( $z$ ) of  $75 \mu\text{m}$  by a microscope objective (N.A. = 0.65) to produce damage filaments. Due to refraction at the air-crystal interface, the effective focus moved to a depth of  $\sim 130 \mu\text{m}$ . The sample was scanned, while irradiating with the laser, in the direction perpendicular to the laser polarization and the pulse propagation, which was carefully aligned with the 10 mm long edge of the sample. In order to fabricate the waveguides, many parallel scans (with  $4 \mu\text{m}$  separation between adjacent scans) were done at different depths of the sample, following the desired geometry (circular) that was programmed in the motorized stage. In order to avoid the shielding and distortion of the incident pulses, the structure was fabricated from large to small depth values. In this way, cladding waveguides with diameter of  $100 \mu\text{m}$  were produced. The scanning velocity and pulse energy were  $700 \mu\text{m/s}$  and  $0.3 \mu\text{J}$ , respectively. Figure 1(a) shows the optical transmission photograph of the circular cladding waveguide obtained for these irradiation conditions, i.e., the one characterized along this work. For comparison, we fabricated a Type II stress-induced DL waveguide in a 6 mm long KTP sample by using the same fs-laser system (see Fig. 1(b) for a microscope image of the cross section) with normal double-line technique and optimized parameters (production details can be seen in [17]).

The propagation loss of the cladding waveguides was determined to be  $\sim 1.7 \text{ dB/cm}$  in the KTP cladding waveguide at  $632.8 \text{ nm}$  by using an end-face coupling system, and no obvious difference was found for the two orthogonal (TE and TM) polarizations. The inscribed surrounding damage tracks were with reduced indices whilst that of the waveguide core remained unchanged. By using

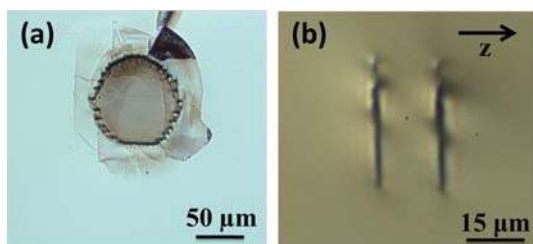


**Figure 1** (online colour at: www.pss-rapid.com) Optical transmission cross-sectional photographs of (a) the circular cladding waveguide and (b) the stress-induced DL KTP waveguide.

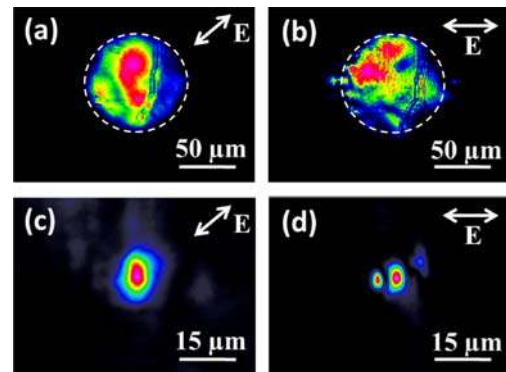


**Figure 2** (online colour at: www.pss-rapid.com) Near-field modal profiles at (a) 1064 nm and (b) 532 nm of the KTP cladding waveguide; modal profiles of the KTP DL waveguide at (c) 1064 nm and (d) 532 nm under pulsed  $1064 \rightarrow 532 \text{ nm}$  green laser SHG configuration. The inserted arrows are the polarizations.

the numerical aperture method [18], we estimated the contrast of the refractive index of the tracks produced with the laser and the central waveguide to be  $\Delta n \approx 0.0035$ . This value is comparable to that previously reported for Nd:YAG cladding waveguides [15].

The SHG experiments were performed by using a similar end-face coupling system as the one used for the guiding mode investigation but now with a Q-switched 1064 nm infrared laser (single pulse energy of  $\sim 80 \mu\text{J}$ , pulse duration  $\sim 11.05 \text{ ns}$ , and repetition rate  $\sim 5 \text{ kHz}$ ) as pump source, and a convex lens (focusing length of  $25 \text{ mm}$ ) as the input coupler. The polarization direction of the 1064 nm beam was set along the  $45^\circ$  direction (i.e., fundamental wave satisfying the  $1/2 e^\omega + 1/2 o^\omega$  for Type II SHG).

Figure 2(a) and (b) show the modal profiles of the pumping fundamental (at 1064 nm) and SH (at 532 nm) beams in the KTP cladding waveguide. As one can see, the cladding waveguide is highly multimode as expected from the large area of the cross section. However, the main electromagnetic energy seems to be concentrated in lower-order modes. This is reasonable because the lower-order modes are more advantageous to higher-order ones on the energy distribution, and we have found that in case of high-intensity beam fields of the pulsed lasers this effect seems to be more obvious. For comparison, we measured the modal profiles of the pump and SH beams in the DL waveguide (see Fig. 2(c) and (d), respectively). It can be seen that for the “double-line” KTP waveguide, the fundamental is in the zero-order mode and SH light is multimodal. It was also noted that the generated SH light exhibited TE polarization (i.e., the SH wave is “e”-light), which is in agreement with the prediction from the bulk prototype configuration Type II ( $e^\omega + o^\omega \rightarrow e^{2\omega}$ ) SHG of KTP crystal.

Figure 3(a) and (b) show the peak power of the output SH wave at 532 nm and the SHG conversion efficiency as a function of the pumped 1064 nm fundamental pulse from the cladding and DL waveguides in KTP, respectively. For the SHG from the cladding structure, the maximum green laser power obtained was  $\sim 0.676 \text{ kW}$  when the 1064 nm

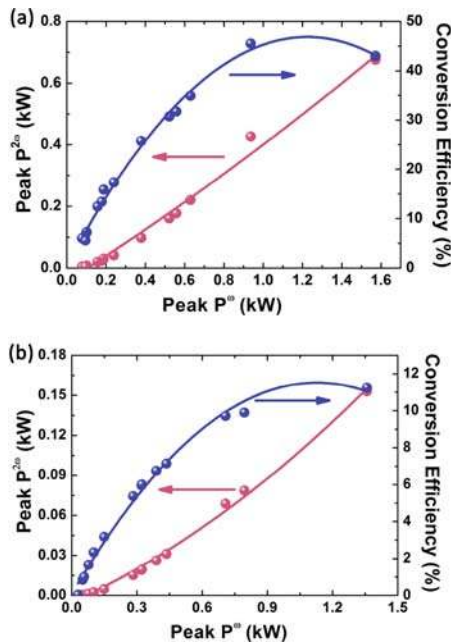


**Figure 3** (online colour at: [www.pss-rapid.com](http://www.pss-rapid.com)) SHG peak output power and conversion efficiency versus the fundamental pump power of (a) the cladding waveguide and (b) the DL KTP waveguide.

pump power was  $\sim 1.572$  kW, resulting in a conversion efficiency of  $\sim 43\%$ . However, the maximum SHG conversion efficiency was achieved at a pump power of  $\sim 0.937$  kW: at this power of the fundamental wave pump, the generated SH signal was  $\sim 0.427$  kW, corresponding to a maximum conversion efficiency as high as  $\sim 45.6\%$ , and to a peak normalized SH conversion efficiency of  $\sim 0.076$   $\% \text{ W}^{-1} \text{ cm}^{-2}$ . The PM SHG conversion efficiency in the KTP cladding waveguide is comparable to that of QPM SHG of green lasers from a fs-laser written PPKTP stress-induced DL waveguide (39.6%) [13] and to that of the PM SHG from the Type I LiNbO<sub>3</sub> (49%) waveguide system [11]. In addition, compared with He-ion-implanted KTP waveguides (25% conversion efficiency), the performance of fs-laser written KTP cladding waveguide seems to be somehow superior for green laser SHG [5]. As we can see from Fig. 3(b), on the DL KTP waveguide the maximum SHG output peak power  $\sim 0.15$  kW was generated at the pumping peak power of  $\sim 1.36$  kW, resulting in a SHG conversion efficiency of  $\sim 11\%$  (corresponding to a normalized conversion efficiency of  $0.025\% \text{ W}^{-1} \text{ cm}^{-2}$ ). Based on the comparison, we found that the SHG in the cladding structure is superior to that produced in the DL waveguide with a three-times magnitude of *normalized* conversion efficiency. The propagation loss of the cladding waveguide ( $\sim 1.7$  dB/cm) was lower than those of the DL structure ( $\sim 2.6$  and  $\sim 3.8$  dB/cm for TE and TM polarization, respectively [17]), which causes an improvement in the SHG efficiency of the cladding waveguide. In addition, the large scale of the cladding waveguide cross section may offer more overlap of the pump and SH beam fields.

Another advantage of the cladding waveguide is that the chosen diameter is comparable with that of a multi-mode fiber, which enables the fabrication of fiber-to-waveguide compact frequency converters. Nevertheless, the stress-induced DL KTP waveguide possesses better modal features with still acceptable SH conversion efficiency.

**3 Summary** We have fabricated large area circular cladding waveguides in KTP nonlinear crystal by using fs-laser inscription. Efficient guided-wave PM SHG at 532 nm has been realized under a pulsed 1064 nm laser pump, reaching the conversion efficiency as high as 45.6%. With comparison to stress-induced DL KTP waveguide, one can conclude that the cladding structure possesses superior SHG performance. Similar cladding structures may be considered as a promising prototype for efficient nonlinear waveguide production in other crystals.

**Acknowledgements** This work was carried out with financial support from the National Nature Science Foundation of China (Grant No. 11111130200), the Spanish Ministerio de Ciencia e Innovación (MICINN) through the Consolider Program SAUUL CSD2007-00013 and project FIS2009-09522. Support from Centro de Láseres-Pulsados (CLPU) is also acknowledged.

## References

- [1] C. Grivas, Prog. Quantum Electron. **35**, 159 (2011).
- [2] M. Ams, G. D. Marshall, P. Dekker, J. Piper, and M. Withford, Laser Photon. Rev. **3**, 535 (2009).
- [3] D. N. Nikogosyan, Nonlinear Optical Crystals: A Complete Survey (Springer, New York, 2005).
- [4] J. D. Bierlein, A. Ferretti, L. H. Brixner, and W. Y. Hsu, Appl. Phys. Lett. **50**, 1216 (1987).
- [5] L. Zhang, P. J. Chandler, P. D. Townsend, Z. T. Alwahabi, S. L. Pityana, and A. J. McCaffery, J. Appl. Phys. **73**, 2695 (1993).
- [6] F. Schrepel, Th. Hoche, J. Ruske, U. Grusemann, and W. Wesch, Nucl. Instrum. Methods B **191**, 202 (2002).
- [7] N. Dong, D. Jaque, F. Chen, and Q. Lu, Opt. Express **19**, 13934 (2011).
- [8] K. M. Davis, K. Miura, N. Sugimoto, and K. Hirao, Opt. Lett. **21**, 1729 (1996).
- [9] J. Thomas et al., Phys. Status Solidi A **208**, 276 (2011).
- [10] J. Burghoff, S. Nolte, and A. Tünnermann, Appl. Phys. A **89**, 127 (2007).
- [11] J. Burghoff, Ch. Grebing, S. Nolte, and A. Tünnermann, Appl. Phys. Lett. **89**, 081108 (2006).
- [12] N. Dong et al., Appl. Phys. Lett. **98**, 181103 (2011).
- [13] S. Zhang, J. Yao, W. Liu, Z. Huang, J. Wang, Y. Li, C. Tu, and F. Lu, Opt. Express **16**, 14180 (2008).
- [14] R. Osellame et al., Appl. Phys. Lett. **90**, 241107 (2007).
- [15] A. Okhrimchuk, V. Mezentsev, A. Shestakov, and I. Ben-ion, Opt. Express **20**, 3832 (2012).
- [16] D. G. Lancaster, S. Gross, H. Ebendorff-Heidepriem, K. Kuan, T. M. Monro, M. Ams, A. Fuerbach, and M. J. Withford, Opt. Lett. **36**, 1587 (2011).
- [17] N. Dong, Y. Tan, A. Benayas, J. V. de Aldana, D. Jaque, C. Romero, F. Chen, and Q. M. Lu, Opt. Lett. **36**, 975 (2011).
- [18] J. Siebenmorgen, K. Petermann, G. Huber, K. Rademaker, S. Nolte, and A. Tünnermann, Appl. Phys. B **97**, 251 (2009).